CORONAVIRUS

Vaccine optimization for COVID-19: Who to vaccinate first?

Laura Matrajt[1]*, Julia Eaton[2†], Tiffany Leung[1†], Elizabeth R. Brown[1,3]

Vaccines, when available, will likely become our best tool to control the COVID-19 pandemic. Even in the most optimistic scenarios, vaccine shortages will likely occur. Using an age-stratified mathematical model paired with optimization algorithms, we determined optimal vaccine allocation for four different metrics (deaths, symptomatic infections, and maximum non-ICU and ICU hospitalizations) under many scenarios. We find that a vaccine with effectiveness ≥50% would be enough to substantially mitigate the ongoing pandemic, provided that a high percentage of the population is optimally vaccinated. When minimizing deaths, we find that for low vaccine effectiveness, irrespective of vaccination coverage, it is optimal to allocate vaccine to high-risk (older) age groups first. In contrast, for higher vaccine effectiveness, there is a switch to allocate vaccine to high-transmission (younger) age groups first for high vaccination coverage. While there are other societal and ethical considerations, this work can provide an evidence-based rationale for vaccine prioritization.

INTRODUCTION

As of 22 September 2020, more than 960,000 people have died because of the ongoing severe acute respiratory syndrome coronavirus 2 (SARS-CoV-2) pandemic (*1*). Different countries have enacted different containment and mitigation strategies, but the world awaits impatiently for the arrival of a vaccine as the ultimate tool to fight this disease and to allow us to resume our normal activities. There are more than 100 vaccines under development (*2*, *3*), with some currently undergoing phase 3 clinical trials (*3*). However, there are many unknowns surrounding a potential vaccine, including how effective it would be, how long it would be protective, how effective it would be in older individuals, how many doses would be immediately available, and how long scaling up the vaccine production would take. Furthermore, should early vaccines have low effectiveness, what are the potential trade-offs between using a low-effectiveness vaccine and waiting for a vaccine with a more desirable vaccine effectiveness (VE)? With the hope of producing a vaccine in the near future comes the difficult task of deciding whom to vaccinate first, as vaccine shortages are inevitable (*4*–*6*). Here, we used a mathematical model paired with optimization algorithms to determine the optimal use of vaccine for 100 combinations of VE and number of doses available under a wide variety of scenarios.

METHODS

Briefly, we developed a deterministic age-structured mathematical model of SARS-CoV-2 transmission with a population stratified into 16 age groups (fig. S1). Because, historically, vaccine is distributed to each state in the United States proportional to its population and the allocation strategy is then determined at the state level (*7*), we chose a state-level model with a population size similar to Washington state and demographics similar to those of the general U.S. population; however, our results are generalizable to other populations.

We assumed that children were less susceptible to infection than middle-aged adults (20 to 65 years old), while older adults (older than 65) were relatively more susceptible (*8*) (we also analyzed a scenario assuming equal susceptibility across age groups; see the Supplementary Materials). We assumed that both natural and vaccine-induced immunity last at least 1 year (our time horizon). At the beginning of our simulations, 20% of the population have already been infected and are immune (additional results for 10, 30, and 40% of the population can be found in Results and in the Supplementary Materials), and all social distancing interventions have been lifted. To keep our results as general as possible, as each state/country will have different vaccination rates, we did not model the vaccination campaigns in the main analysis. Hence, we assumed that at the beginning of our simulations, vaccination has been carried out and that vaccinated individuals have reached the full protection conferred by the vaccine. However, we also analyzed, in a separate scenario, how optimal allocation strategies changed when we modeled vaccination campaigns explicitly. Here, we consider that frontline health care workers and other essential personnel (e.g., firefighters and police) who should obviously be prioritized have already been vaccinated.

For the main analysis, we considered a vaccine having an effect of reducing susceptibility to infection (referred to VE throughout the text) only. In addition, as a separate analysis, we considered a vaccine that would also reduce the probability of COVID-19 disease (referred to as VE_{COV} below). This effect against COVID-19 disease was modeled as a combination of the VE to prevent infection and the VE to prevent disease-given infection. Because current vaccine clinical trial protocols have an expected VE against COVID-19 disease of 60% (*9*, *10*), for this analysis, we set $VE_{COV} = 60$ while varying the relative contributions of the other two vaccine effects (see the Supplementary Materials for full description).

For the vaccine optimization, we collated the 16 age groups into five vaccination groups: children (aged 0 to 19), adults between 20 and 49 years old, adults between 50 and 64 years old, adults between 65 and 74 years old, and those 75 and older. This stratification reflects our current knowledge of disease severity and mortality based on age (*11*, *12*).

We developed an optimization routine that combined a coarse global search algorithm with a fast optimizer to explore the entire space of possible combinations of vaccine allocation. We compared the optimal allocation strategy given by the optimizer to a pro rata allocation, where the vaccination coverage to each vaccination group is distributed proportionally to population size in each group. We

[1]Vaccine and Infectious Disease Division, Fred Hutchinson Cancer Research Center, Seattle, WA, USA. [2]University of Washington, Tacoma, WA, USA. [3]Department of Biostatistics, University of Washington, Seattle, WA, USA.
*Corresponding author. Email: laurama@fredhutch.org
†These authors contributed equally to this work.

considered VE ranging from 10 to 100% and vaccination coverage ranging from 10 to 100% of the total population. We evaluated four objective functions reflecting different metrics of disease burden that could be considered by decision makers: minimization of the total number of symptomatic infections, total number of deaths, number of cases requiring hospitalization [non–intensive care unit (ICU)] at the epidemic peak, and number of cases requiring ICU hospitalization at the epidemic peak. We chose to minimize symptomatic infections as a key metric because symptomatic individuals are the ones who are easier to identify and, presumably, particular interventions will be targeted to this group. In addition, minimizing symptomatic individuals minimizes the transmission of SARS-CoV-2, and this is in line with current vaccine trials end points (*9*, *10*). The last two objective functions were chosen because hospital bed (non-ICU and ICU) occupancy is a key metric currently used to determine county/state/country readiness to move between different intervention strategies. Here, we used the total number of licensed ICU beds in Washington state and its current goal of staying below 10% of hospital beds occupied by COVID-19 cases (*13*, *14*) as references when interpreting our results. Full details of the methods can be found in the Supplementary Materials.

RESULTS

Epidemic mitigation and containment

Our model suggests that, for a basic reproduction number $R_0 = 3$, herd immunity will be achieved once 60% of the population is infected (equivalently 40% vaccinated with a perfect vaccine under the optimal allocation strategy for minimizing infections assuming 20% of the population has immunity already) (Figs. 1J and 2A and fig. S2).

The epidemic can be substantially slowed with any vaccine with a VE ≥50%, as long as a majority of the population is vaccinated (Figs. 1E and 2A), and more than 50% of deaths could be averted (in comparison to no vaccination and no nonpharmaceutical intervention) with as little as 35% of the population optimally vaccinated (Fig. 2, A and B). If VE = 60%, then the epidemic is completely contained if we optimally vaccinate 70% of the population (or 50% for higher VE = 70%) (Figs. 1, F and I, and 2A). In our model, only vaccines with VE ≥50% can maintain the number of non-ICU hospitalizations below the established goal (≤10% hospital bed occupancy by patients with COVID-19) and can prevent an overflow of the ICUs. With VE = 60%, optimally vaccinating 54% satisfies both hospital bed occupancy goals (Fig. 2, C and D, and figs. S3F and S4F), compared with 67% under the pro rata allocation (figs. S5 to S9). The optimal allocation strategy outperforms the pro rata allocation most under low vaccine availability, with a maximum difference of 32% deaths averted (for VE = 100% and with enough vaccine to cover 20% of the population) and 32% symptomatic infections averted (for VE = 60% and vaccination coverage of 60%) when compared with a pro rata allocation strategy (Fig. 3 and figs. S5 and S10). As VE increases, both strategies tend to perform similarly as vaccination coverage increases (Fig. 3 and figs. S5 and S10).

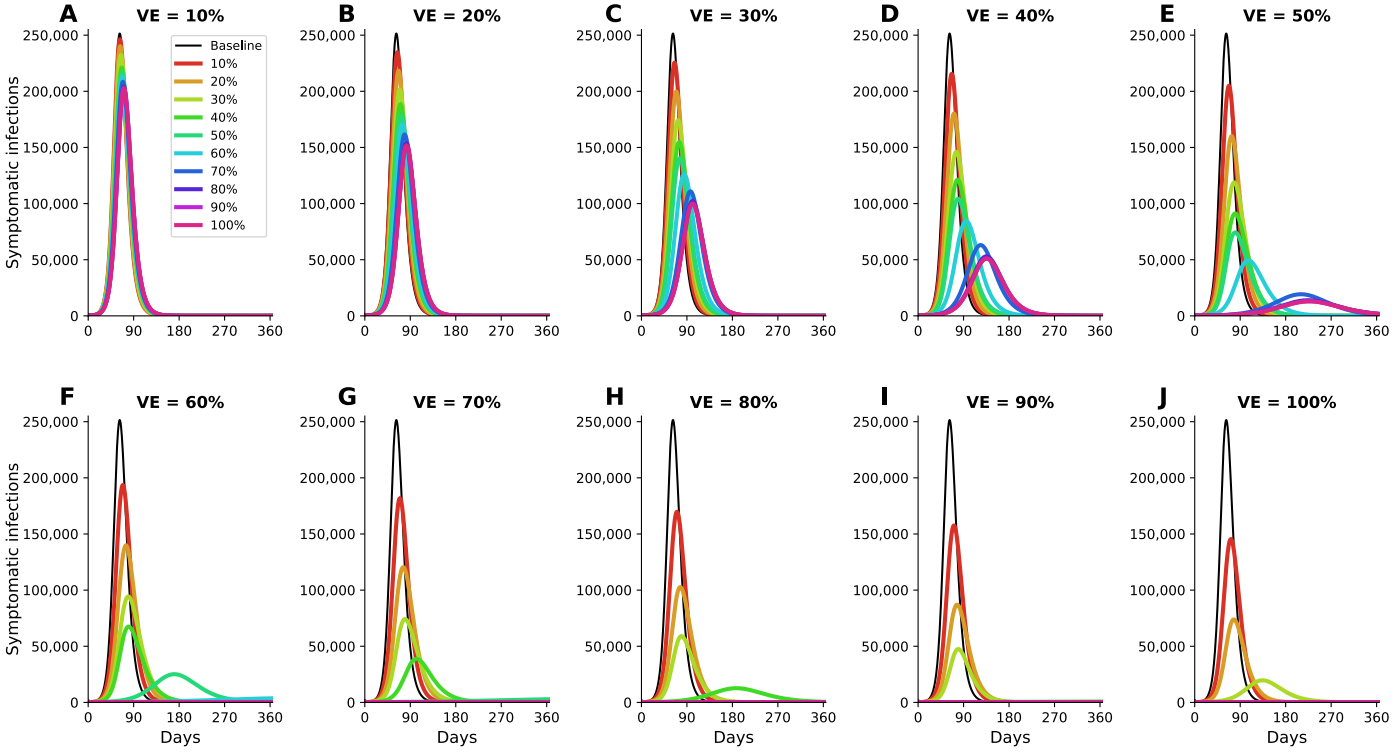

Fig. 1. Simulated prevalence of symptomatic infections. Simulated prevalence of symptomatic COVID-19 infections for VE ranging from 10% (**A**) to 100% (**J**) in 10% increments. For each VE and each vaccination coverage, the optimal vaccine allocation for minimizing symptomatic infections was used in these simulations. Colors represent different vaccination coverage, ranging from 0% (black, "baseline") to 100% (magenta). For clarity, we present here epidemic curves for the main set of parameters only and show a complete figure with uncertainty bounds in fig. S2.

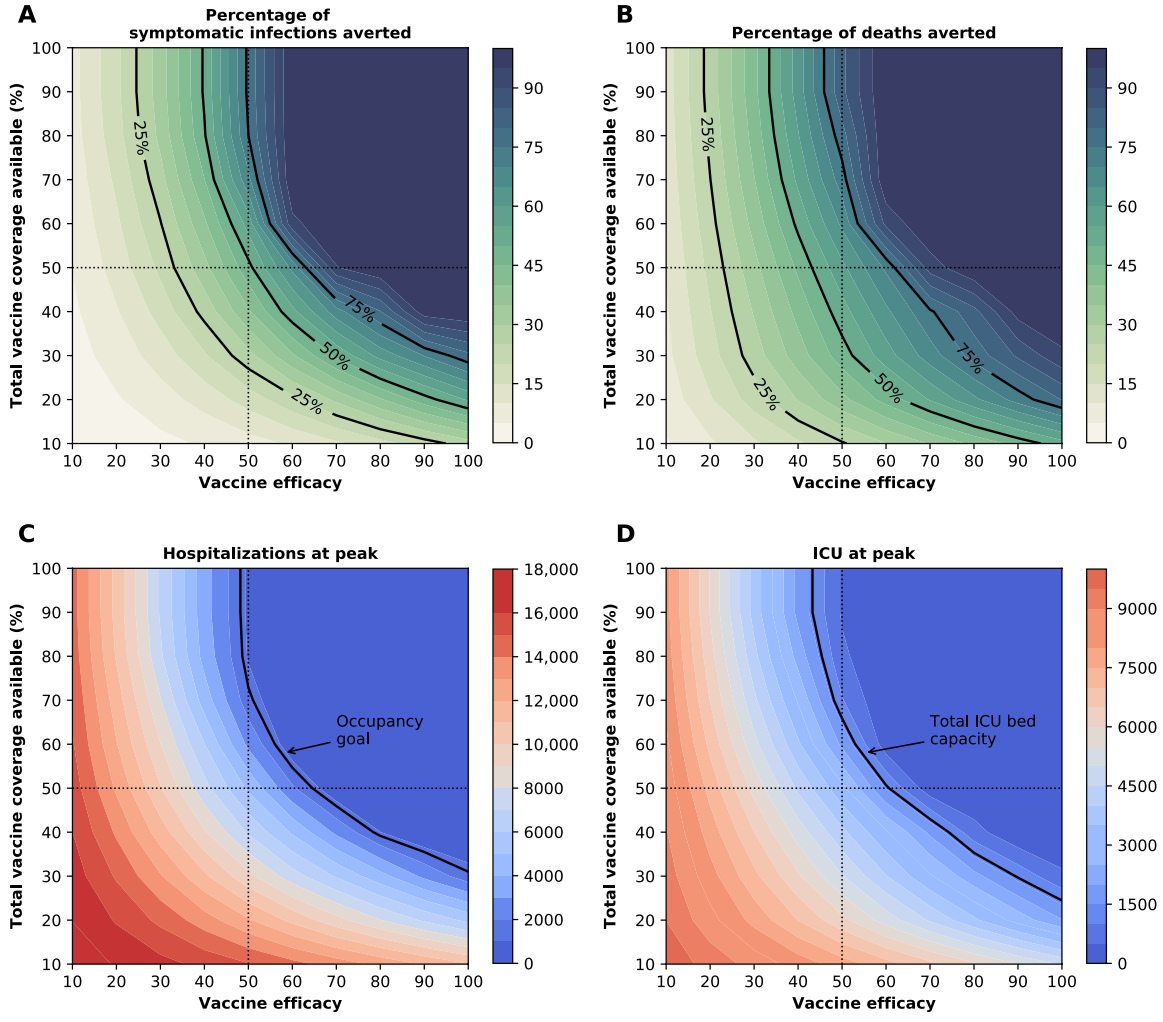

Fig. 2. Four key metrics of COVID-19 burden under optimal distribution of vaccine. Percentage of symptomatic infections (**A**) and deaths (**B**) averted, and number of maximum non-ICU (**C**) and ICU (**D**) hospitalizations as a function of VE and vaccination coverage (total vaccine available as a percentage of the population). The dotted lines correspond to VE = 50% and vaccine available to cover 50% of the population. The isoclines indicate the current goal for Washington state having 10% of licensed general (non-ICU) hospital beds occupied by patients with COVID-19 in (C) and total ICU licensed hospital beds in Washington state in (D).

Optimal vaccine allocation changes with VE and vaccination coverage

The optimal allocation strategy to minimize deaths is identical for VE between 10 and 50%: With low vaccination coverage, it is optimal to allocate vaccine first to the highest-risk group (people more than 75 years old) and then to the younger vaccination groups as more vaccine becomes available (Fig. 4, A to E). In contrast, there is a threshold phenomenon observed for VE ≥60%: For low coverage, the optimal allocation is still to vaccinate the high-risk groups first, but when there is enough vaccine to cover roughly half of the population (60% for VE = 60%, 50% for VE = 70%, and 40% for VE≥80%), there is a switch to allocate vaccine to the high-transmission groups first (those aged 20 to 50 and children in our model). This is because directly vaccinating those who are driving the epidemic results in a much slower epidemic curve and, hence, in fewer deaths (Fig. 1, F to H). As more vaccine becomes available, the optimizer allocates it to high-risk groups again (Fig. 4, F to J).

Optimal vaccine allocation differs for different objective functions

Next, we investigated how the optimal allocation strategy changed for different objective functions and present results for VE = 60%. The optimal vaccine allocation for the four objectives differed the most when fewer vaccines are available (enough vaccine to cover less than 30% of the total population). When minimizing symptomatic infections and peak non-ICU hospitalizations, priority was given to the younger vaccination groups, as they have the most contacts in our model and, hence, drive transmission (Fig. 5, A and B, and figs. S11 and S12). As we move toward more severe outcomes (ICU hospitalizations at peak and deaths), for which older individuals are most at risk, the optimal allocation strategy shifts toward those vaccination groups (Fig. 5, C and D, and fig. S13). Once more vaccine becomes available, the optimal allocation strategies are very similar for all objective functions. They are nearly identical for all the objective functions when there is enough vaccine to cover 60 and 70% of

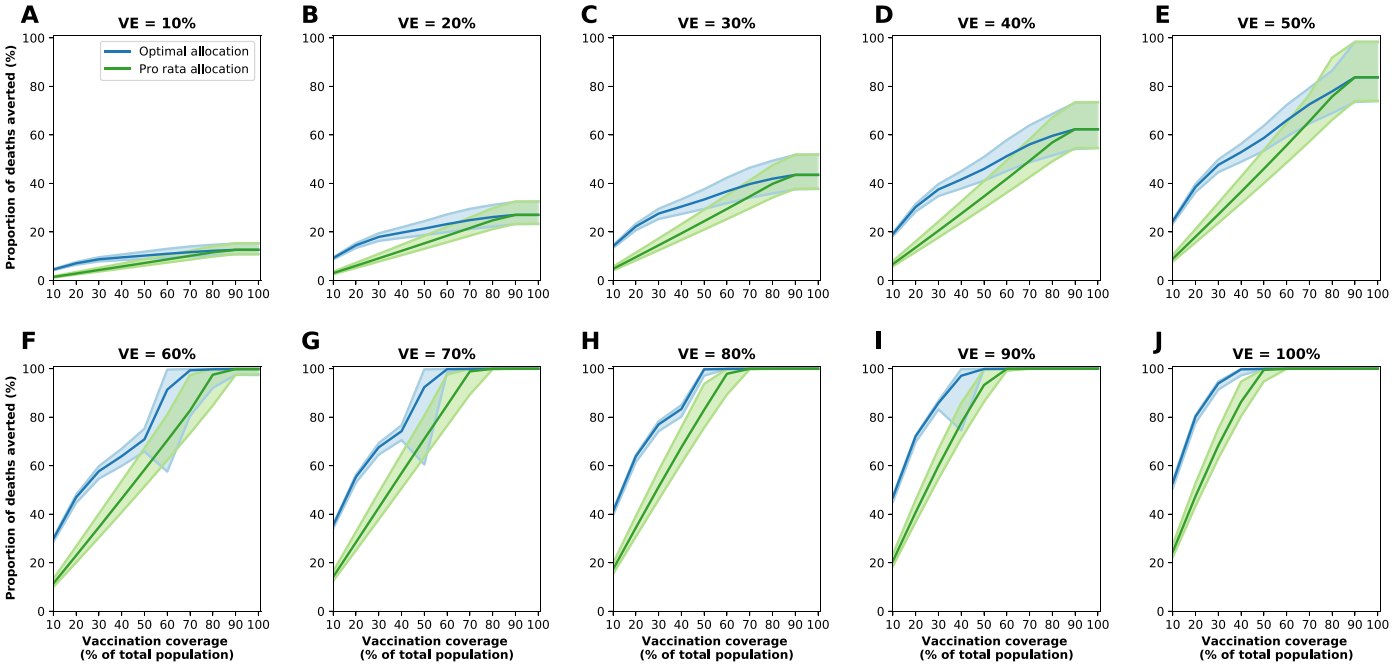

Fig. 3. Percentage of deaths averted under the optimal and the pro-rata strategies for different VE. Percentage of deaths averted for the optimal allocation strategy (blue) and the pro rata strategy (green) for VE ranging from 10 (**A**) to 100% (**J**) in 10% increments and vaccination coverage ranging from 10 to 100% of the total population. The shaded areas represent results of the 1000 simulations with the top and bottom 2.5% simulations removed.

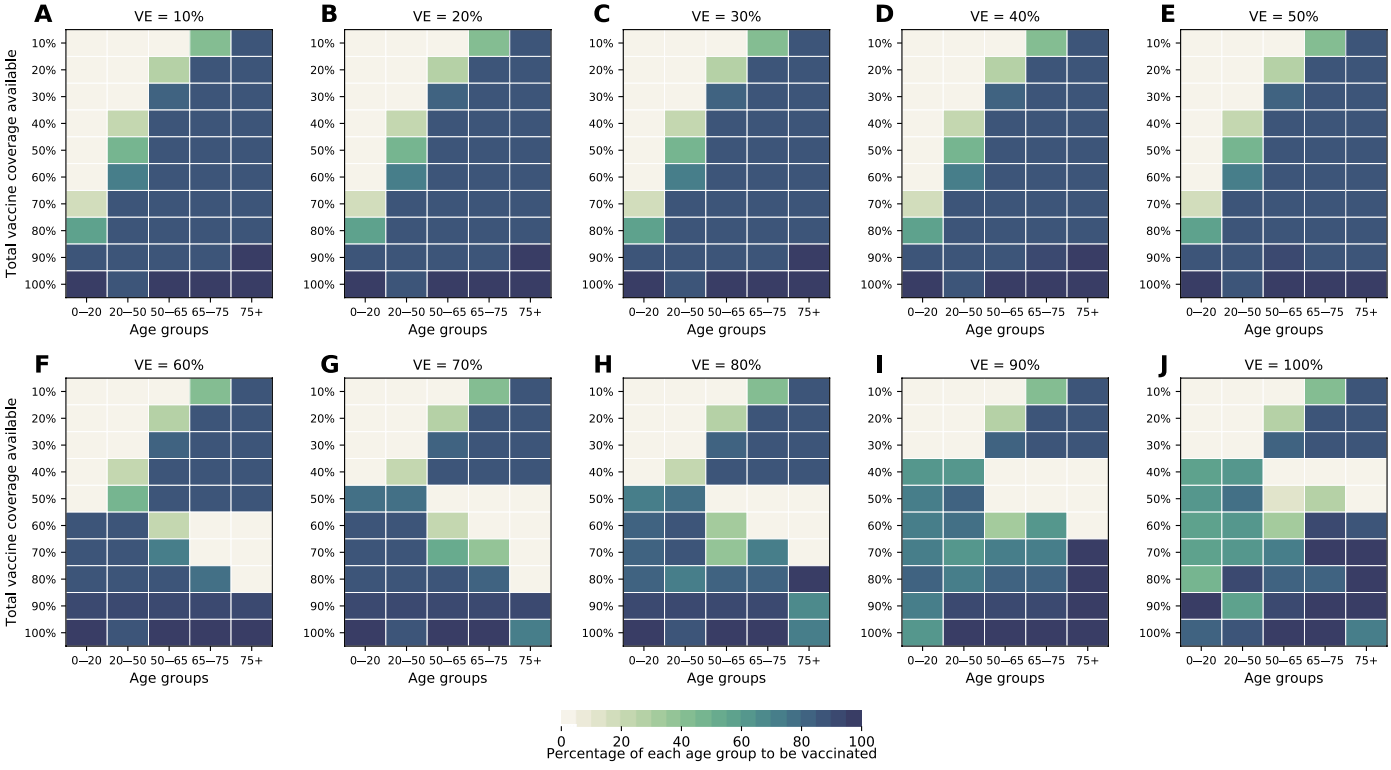

Fig. 4. Optimal allocation strategies to minimize deaths for different VE. Optimal allocation strategies for minimizing deaths for VE ranging from 10 (**A**) to 100% (**J**) in 10% increments (additional figures for minimizing symptomatic infections, number of non-ICU hospitalizations at peak, and number of ICU hospitalizations at peak are given in the Supplementary Materials). For each plot, each row represents the total vaccination coverage available (percentage of the total population to be vaccinated), and each column represents a different vaccination group. Colors represent the percentage of the population in a given vaccination group to be vaccinated.

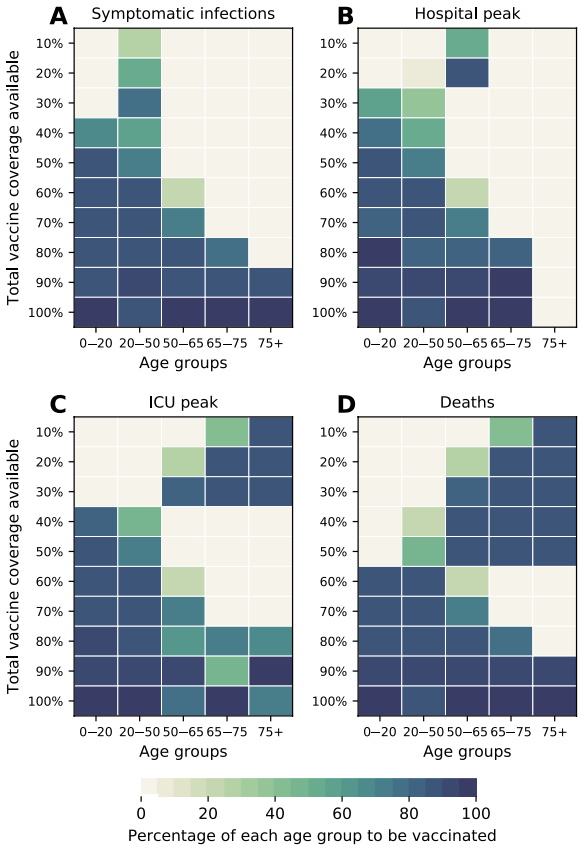

Fig. 5. Optimal allocation strategies for all objective functions analyzed. Optimal allocation strategies for minimizing: Symptomatic infections (**A**), number of non-ICU hospitalizations at peak (**B**), number of ICU hospitalizations at peak (**C**), and total number of deaths (**D**). Here, we assumed VE = 60%. For each plot, each row represents the total vaccination coverage available (percentage of the total population to be vaccinated), and each column represents a different vaccination group. Colors represent the percentage of the population in a given vaccination group to be vaccinated.

the population. For high coverage, the optimal allocation strategies for all objective functions shifted toward the high-transmission groups. Of note, we did not impose the optimizer to use all the available vaccine. As a result, the optimizer found allocation strategies using less than the total vaccine available while performing equally well. This was very prominent when VE and vaccination coverage were very high. For example, when minimizing peak ICU hospitalizations and VE = 90%, the optimizer used vaccine to cover 75% of the population even though there was vaccine available to cover the entire population. This is expected because complete containment is attained once a high proportion of the population is vaccinated, and any vaccine used above that threshold will result in the same mathematical outcome.

Optimal vaccine allocation assuming VE against COVID-19 disease (VE_{COV})

In this section, we considered a vaccine that, in addition to reducing the probability of acquiring infection, would reduce the probability of COVID-19 disease (see the Supplementary Materials for full details). We considered VE_{COV} = 60%, in line with expected VE in the current trial protocols (*9*, *10*). The optimal allocation strategies assuming VE_{COV} = 60% are nearly identical to the ones without this effect (Fig. 6 and figs. S14 to S16). As expected, including this effect against COVID-19 disease has a huge impact on symptomatic infections and hospitalizations, even when this vaccine is marginally effective against preventing infection (Fig. 7). For example, if VE = 10%, then it can prevent 50% of the symptomatic infections when we optimally vaccinate 64% of the population (Fig. 7A). Furthermore, for this VE and this vaccination coverage, peak hospitalizations are substantially reduced (6840 and 3392 non-ICU and ICU hospitalizations, respectively; Fig. 7, B and C) when compared with a vaccine without an effect in COVID-19 disease (15,091 and 8405 non-ICU and ICU hospitalizations, respectively; Fig. 2, B and C).

Optimal vaccine allocation as a function of preexisting immunity to SARS-CoV-2

As the COVID-19 pandemic dynamics have been markedly different across the globe, we expect to see a range of population-level naturally acquired immunity when vaccination campaigns start. Hence, we investigated the optimal use of vaccine with 10, 30, and 40% of the population already immune at the beginning of the simulations. For all of these scenarios, the same pattern is observed when minimizing deaths: For low coverage, it is optimal to allocate all of the vaccine to the high-risk groups; for higher coverage, the optimal vaccination strategy switches to allocate more vaccine to the high-transmission groups. This threshold, however, varies with the degrees of preexisting immunity in the population. When only 10% of the population has natural immunity, the switch occurs at 80% vaccination coverage, but when 40% has natural immunity, the threshold is observed at 40% vaccination coverage (Fig. 8).

In addition, under low preexisting immunity to SARS-CoV-2, the optimal strategy favors vaccinating the older vaccination groups (Fig. 8A), while under higher preexisting immunity, the optimal allocation strategy tends to distribute vaccine more evenly across vaccination groups (Fig. 8D).

Modeling the vaccination campaign

In this section, we modeled the vaccination campaign and determined the optimal vaccine allocation. We extended our time horizon to 2 years and considered administering 75,000, 150,000, or 300,000 doses of vaccine per week. This corresponds to vaccinating the entire population in 101, 50, or 25 weeks, respectively. The first vaccination rate was chosen to roughly match the vaccination rate during the 2009 H1N1 pandemic in the United States (0.87% of the population weekly) (*15*). Note that to avoid confounding, as in the rest of this work, we did not assume any social distancing intervention. Similar to previous results, when the vaccination campaign is modeled, the optimal vaccine allocation strategies were very different depending on the objective function: While the older age groups are prioritized when minimizing deaths and maximum ICU hospitalizations (Fig. 9), the optimizer allocated vaccine to younger age groups when minimizing symptomatic infections or maximum non-ICU hospitalizations (fig. S17). Furthermore, older age groups were prioritized when vaccination rate was slow (75,000 doses administered per week, when minimizing deaths and ICU peak hospitalization). For faster vaccination campaigns, the optimizer allocated vaccine to younger age groups in addition to the older age groups (Fig. 9). There were also some important differences. First, for any VE and any vaccination rate, we did not observe any threshold in vaccination coverage. In addition, because the time frame of the vaccination campaigns occurs at a much slower speed than the epidemic, most of the vaccines under

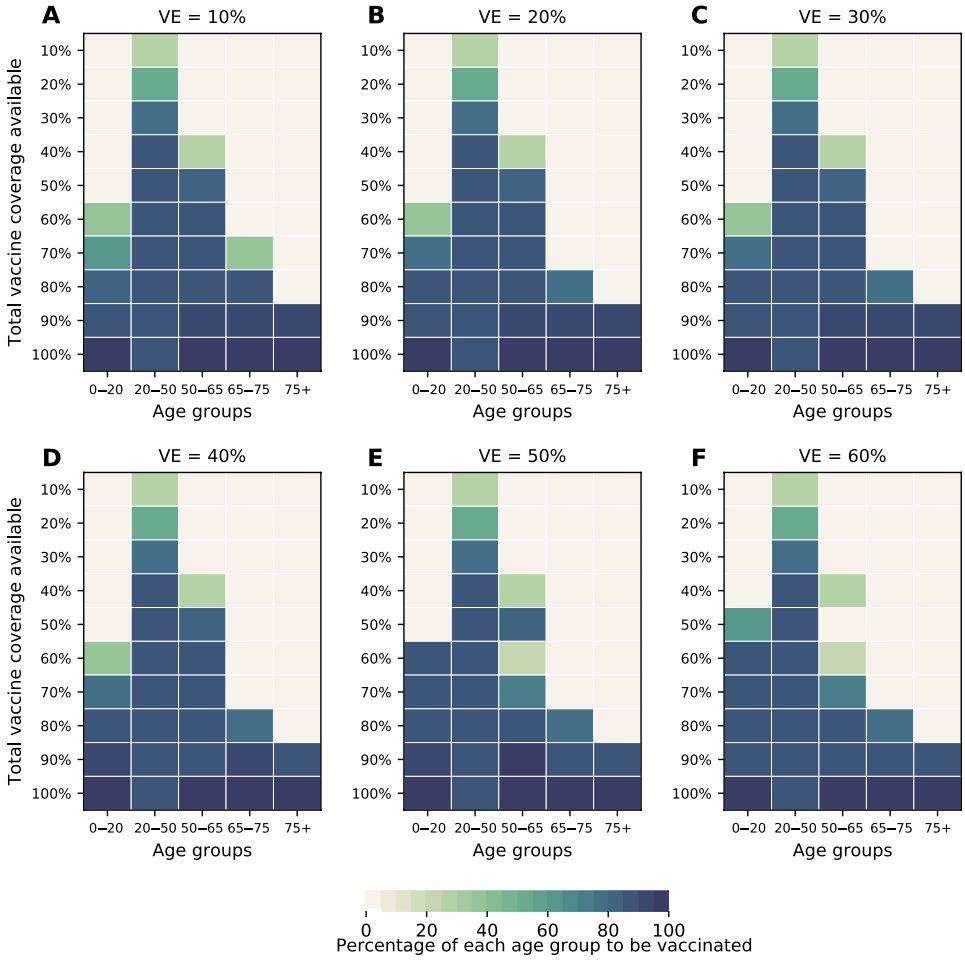

Fig. 6. Optimal allocation strategies for different VE with a vaccine including an effect against COVID-19 disease. Optimal allocation strategies for minimizing total symptomatic infections for VE ranging from 10% (**A**) to 60% (**F**) in 10% increments for VE_{COV} = 60%. For each plot, each row represents the total vaccination coverage available (percentage of the total population to be vaccinated), and each column represents a different vaccination group. Colors represent the percentage of the population in a given vaccination group to be vaccinated.

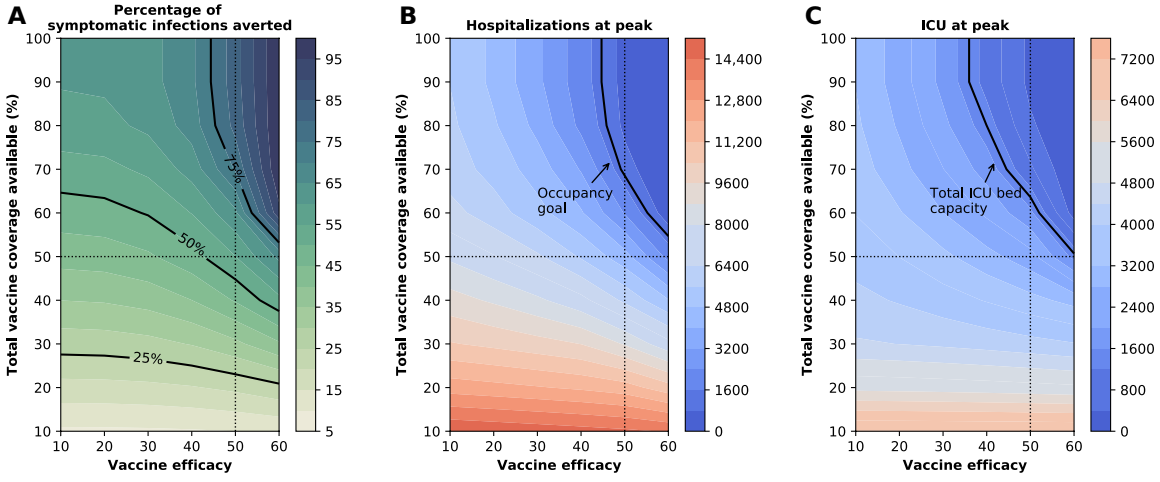

Fig. 7. Three key metrics of COVID-19 burden under optimal distribution of vaccine for VE_{COV} = 60%. Percentage of symptomatic infections averted (**A**) and number of maximum non-ICU (**B**) and ICU (**C**) hospitalizations as a function of VE and vaccination coverage (total vaccine available as a percentage of the population). The dotted lines correspond to VE = 50% and vaccine available to cover 50% of the population. The isoclines indicate the current goal for Washington state having 10% of licensed general (non-ICU) hospital beds occupied by patients with COVID-19 in (B) and total ICU licensed hospital beds in Washington state in (C).

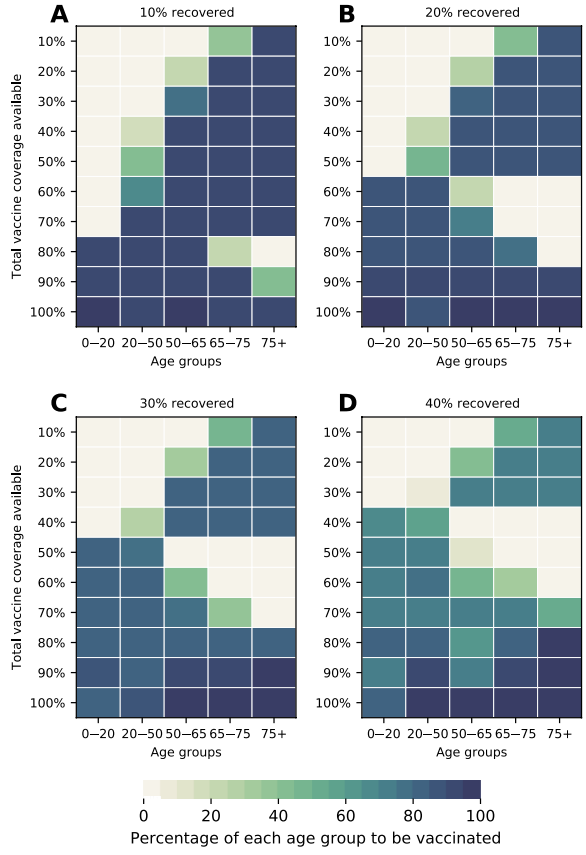

Fig. 8. Optimal allocation strategies for minimizing deaths assuming different levels of pre-existing immunity in the population. Optimal allocation strategies for minimizing deaths assuming 10% (**A**), 20% (**B**), 30% (**C**), and 40% (**D**) of the population has natural immunity to COVID-19 at the start of the simulations. Here, we assumed VE = 60%. For each plot, each row represents the total vaccination coverage available (percentage of the total population to be vaccinated), and each column represents a different vaccination group. Colors represent the percentage of the population in a given vaccination group to be vaccinated.

this scenario are given after the epidemic (this was especially true when considering the 75,000 campaign). This resulted in optimal allocation strategies that, for a given VE, were identical beyond a certain vaccination coverage (Fig. 9 and fig. S17), and the measured outcomes did not improve beyond that coverage (fig. S18). This points to the fact that even in the very optimistic scenario of having a highly efficacious vaccine given at very high rates, additional interventions would be necessary to control the epidemic while the vaccination campaign takes place.

Robustness of optimal allocation strategies around major parameters

One-way robustness analysis

We explored the robustness of the optimal allocation strategies around key features of the transmission and natural history of SARS-CoV-2. For each of these features, we investigated how changing that particular parameter would change the optimal allocation strategy.

Susceptibility to infection. Because the effect of age on susceptibility to SARS-CoV-2 infection remains unclear, we compared the optimal allocation strategy under the assumption of differential susceptibility, as suggested in (*8*, *16*) (presented throughout the text), to one assuming equal susceptibility across age groups (figs. S19 to S22), as suggested in (*17*, *18*). The optimal allocation strategies under both equal and differential susceptibility were remarkably consistent, but, as expected, assuming equal susceptibility resulted in strategies allocating slightly more vaccine to children (assuming equal susceptibility) as VE increases (VE ≥60) and more vaccine becomes available (coverage to vaccinate 70% or higher) (figs. S19 to S22). The major differences were observed when minimizing peak non-ICU hospitalizations for low VE and low vaccination coverage [less than, assuming equal susceptibility resulted in favoring adults aged 50 to 65 over younger adults (fig. S21)].

Susceptibility to symptomatic disease. While we know that children are much less susceptible to develop severe disease (*19*), the role of age in the probability of developing any kind of COVID-19 symptoms remains currently unclear. Hence, we compared optimal allocation strategies assuming equal probability of all age groups to develop symptoms (presented throughout the text), as suggested in (*19*, *20*), to ones assuming different probabilities by age (children being less susceptible and older adults being more susceptible), as suggested in (*21*). The optimal allocation strategies for minimizing deaths and peak ICU are very consistent (figs. S23 and S24), but, as expected, we observed some changes when minimizing symptomatic infections and peak non-ICU hospitalizations (figs. S25 and S26). When we minimized symptomatic infections, the optimal allocation strategies were very similar for vaccines with VE ≥60. For lower VE, the optimal allocation strategies tended to favor more the middle- and older-age adult groups (fig. S25). When minimizing maximum non-ICU hospitalizations, the optimal allocation strategies were nearly identical for high vaccination coverage (≥70%) but switched to adults aged 50 to 75 (as opposed to younger adults) if vaccination coverage is lower (fig. S26).

Basic reproduction number R_0. Many regions in the world have controlled the epidemic using social distancing interventions and have reduced the effective reproduction number R_t to hover around 1. Hence, we analyzed the optimal allocation strategies in this section with R_0 set to 1.5, 2, and 2.5, assuming still that at the beginning of our simulations, 20% of the population have been infected and are now recovered. For minimizing deaths and ICU peak hospitalizations, when $R_0 = 1.5$, the optimal allocation strategy favors vaccinating children for low VE (Fig. 10A and fig. S27), is more equally distributed if VE = 60%, and favors vaccinating the older age groups for higher VE (Fig. 10, D and G). If $R_0 = 2$, then we observe the same threshold phenomenon described for higher R_0, but at a lower VE: For VE = 30%, the optimal use of vaccine is to allocate it to high-risk groups under low vaccine coverage and to the younger groups once there is enough vaccine to cover 60% of the population. As VE is higher, this threshold moves up (Fig. 10, C, G, and K). Last, for $R_0 = 2.5$, the optimal allocation strategy is identical to the one for $R_0 = 3$. For minimizing symptomatic infections and non-ICU peak hospitalizations, the optimal allocation strategies were more homogeneous, favoring more the younger age groups in alignment with the results presented above (figs. S28 and S29). Note here that social distancing interventions have kept the effective reproduction number low, but that, if those measures are lifted, then R_t would go up again. Hence, any vaccination program should take this into account.

Distribution of preexisting immunity in the population. Here, we assumed a different distribution of preexisting immunity in the population. For this section of the analysis, we ran the simulations without any vaccination until the recovered compartments reached

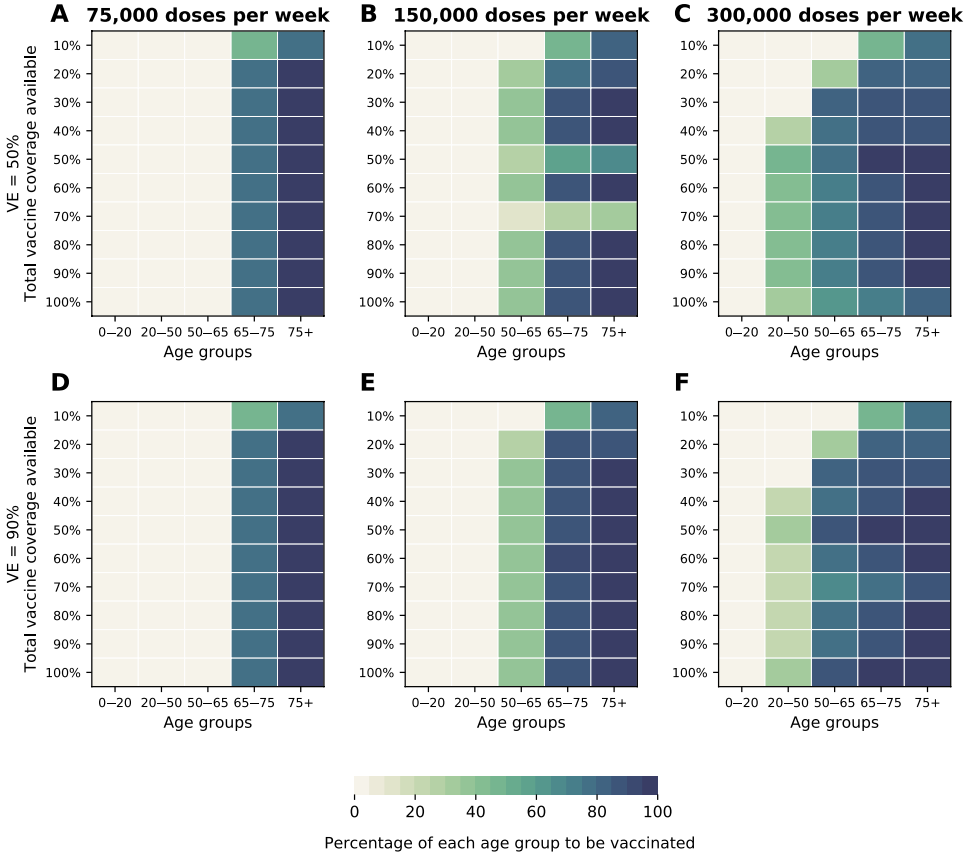

Fig. 9. Optimal allocation strategies for minimizing deaths assuming different vaccination rates. Optimal allocation strategies for minimizing deaths for two VE = 50% (**A** to **C**) and 90% (**D** to **F**) and for three different vaccination rates: 75,000 (A and D), 150,000 (B and E), and 300,000 (C and F) vaccine doses administered per week. For each plot, each row represents the total vaccination coverage available (percentage of the total population to be vaccinated), and each column represents a different vaccination group. Colors represent the percentage of the population in a given vaccination group to be vaccinated.

20% of the population. We then used this composition of the population as the initial distribution of preexisting immunity (this composition will depend on the contact matrix and the demographics used). The optimal allocation strategies were very similar to those obtained in the main analysis, with some notable differences. First, under this scenario, the optimal allocation strategies tended to protect vaccination groups in full before prioritizing other groups. This was very apparent when minimizing deaths or peak ICU hospitalizations: For low VE (irrespective of vaccination coverage) or high VE but low vaccination coverage, the optimal allocation strategies prioritized the highest-risk age groups (individuals aged 65 to 75 and those more than 75 years old) to get fully vaccinated before allocating to other groups (figs. S30 and S31). Second, the threshold observed when minimizing deaths occurred at higher vaccination coverage under this scenario. For example, if VE = 60%, then this threshold occurs when there is enough vaccine to cover 70% of the population (fig. S30, F to J). Last, when minimizing symptomatic infections or non-ICU peak hospitalizations, the optimal allocation strategies shifted away from young adults toward adults in the 50-to-65 vaccination groups (figs. S32 and S33).

Duration of the incubation period. On the basis of the early studies (*17*, *22*–*24*), we presented results assuming an incubation period of 5.1 days. However, a more recent study (*25*) has suggested that the incubation period for COVID-19 might be longer (7.76 days). We found no difference in the optimal allocation strategies assuming this longer incubation period (fig. S34).

Number of current infections. We compared the optimal allocation strategies when the simulations were started with a higher number of infected individuals (10,000 current infections). This would reflect a situation where the epidemic is in full exponential growth when vaccination becomes available. The optimal allocation strategy was unexpectedly robust under this scenario, with nearly identical allocation strategies for all objective functions (fig. S35).

Multiway robustness analysis

In addition, we selected four parameters (R_0, proportion of infections that are asymptomatic, relative infectiousness of asymptomatic infections, and relative infectiousness of presymptomatic infections) for which there is the most uncertainty and reran the optimization routine for several combinations of them (full details in the Supplementary Materials). The optimal allocation strategies were very robust under this analysis (Supplemental Files SF1 to SF4).

DISCUSSION

The COVID-19 pandemic has devastated families and societies around the world. A vaccine, when available, would most likely become our best tool to control the spread of SARS-CoV-2. However, in the short term, even in the most optimistic scenarios, vaccine production would likely be insufficient. In this work, we paired a mathematical model of SARS-CoV-2 transmission with optimization algorithms to determine optimal vaccine allocation strategies. Given

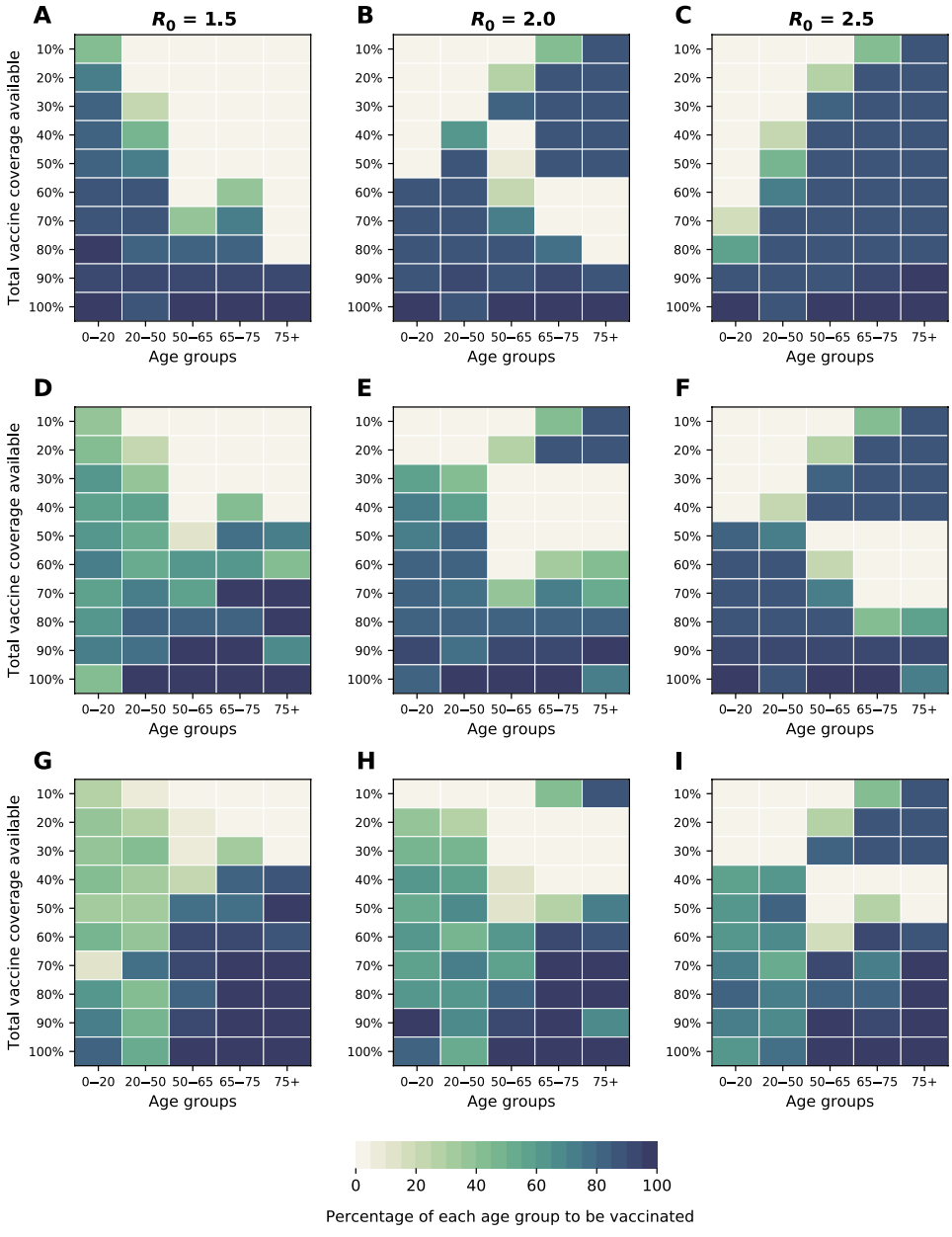

Fig. 10. Optimal allocation strategies for minimizing deaths for different values of R_0. Optimal allocation strategies for minimizing deaths for three different VE: 30% (**A** to **C**), 60% (**D** to **F**), and 90% (**G** to **I**) for three different values of R_0 = 1.5, 2, and 2.5 (additional figures for minimizing symptomatic infections, number of non-ICU hospitalizations at peak, and number of ICU hospitalizations at peak are given in the Supplementary Materials). For each plot, each row represents the total vaccination coverage available (percentage of the total population to be vaccinated), and each column represents a different vaccination group. Colors represent the percentage of the population in a given vaccination group to be vaccinated.

the current uncertainties surrounding such a vaccine (we do not yet know whether and when this vaccine would be available, how efficacious it will be, or the number of doses immediately available), we explored 100 combinations of VE and vaccination coverage under a wide variety of scenarios minimizing four metrics of disease burden.

Our results suggest that, assuming R_0 = 3, any vaccine with medium to high effectiveness (VE ≥50%) would be able to considerably slow the epidemic while keeping the burden on health care systems manageable, as long as a high proportion of the population is optimally vaccinated. Moreover, once VE = 70%, full containment of the epidemic would be possible. This is in agreement with vaccine modeling studies (*26*, *27*). Furthermore, we showed that much can be achieved even with low vaccination coverage; With medium VE, more than half of deaths can be averted by optimally vaccinating only 35% of the population. When minimizing deaths, for low VE and a low supply of vaccine, our results suggest that vaccines should be given to the high-risk groups first. For high VE and high vaccination coverage, the optimal allocation strategy switched to vaccinating the high-transmission groups (younger adults and children). This remained true under equal or reduced susceptibility to infection for children, pointing to the importance of children as key players in disease transmission. This finding is consistent with

previous work for other respiratory viruses (*28*–*30*) that found that protecting the high-transmission groups indirectly protects the high-risk groups and is the optimal use of resources.

Furthermore, the optimal allocation strategies were identical when we considered a vaccine that would also reduce symptomatic infections, but the impact of such a vaccine would of course be greater in reducing COVID-19 disease and health care burden. Our results show that even if this vaccine had a marginal effect in preventing infection, it would still be very beneficial to reduce the number of hospitalizations and symptomatic infections. It is expected that once a vaccine is proven to be effective, more information about its mechanisms of action, including how it affects the viral load trajectory and the relationship between that trajectory and infectiousness, will be available, allowing us to expand and refine our projections.

Here, we used mathematical optimization to determine the optimal vaccine allocation and, by design, did not impose any restrictions in the allocation strategies.

However, in practice, implementation of optimal strategies must also account for other factors (ethical, political, and societal). When large quantities of vaccine are available, a feasible solution could involve first vaccinating the high-risk groups and then allocating the remaining vaccine to the high-transmission groups.

This study has several limitations. Our model assumes that both natural and vaccine-acquired immunity will last for at least 1 year. We do not yet know how long immunity against SARS-CoV-2 will last. There is some evidence that neutralizing antibodies become undetectable a few weeks following infection (*31*), although it is unclear how this correlates with immunity. If immunity were short-lived, then these results would only be applicable for that duration. Furthermore, we assumed that asymptomatic and symptomatic infections would confer equal immunity. However, it is conceivable that asymptomatic infections might result in a weaker immune response (*32*). We chose four metrics of disease burden to minimize. However, other metrics, such as minimization of asymptomatic infections, or a combination of all of these metrics might be the key to stop the spread of the epidemic. We have identified optimal allocation strategies, and once more information about a vaccine characteristics is known, validating our allocation strategies with more complex models is welcome. To avoid confounding effects from different interventions, we optimized vaccine allocation assuming no social distancing interventions in place. In reality, vaccination, at least at the beginning, would take place while some social distancing interventions remain in effect. Under those circumstances, we would need less vaccine to control the epidemic. In that sense, our results are conservative. To keep the optimization from being unreasonably long, our model assumes that vaccination is given all at once and does not capture geographical differences or other heterogeneities.

We used mortality and hospitalization rates published by Ferguson *et al.* (*12*) that were based on the epidemic in Wuhan, China, but these rates may vary vastly in different regions. In particular, it is now known that certain underlying conditions (e.g., obesity, diabetes, and heart disease) are important risk factors for developing severe COVID-19 hospitalization and death. As the population makeup of individuals with underlying conditions can be very different in different countries, it is then key to determine region-based estimates of COVID-19–related hospitalizations and deaths, so that models can be adequately parameterized. Furthermore, we compared modeled peak hospitalizations to current state goals for hospital bed occupancy, but it is possible that a lower VE or a lower vaccination coverage could achieve the same goals, because deterministic models tend to overestimate the transmission dynamics. We computed the optimal allocation strategies using age as the sole risk factor. However, other factors, such as occupation, have been linked to an increased risk of acquisition and severe disease (*33*, *34*). Furthermore, several studies (*35*, *36*) have shown that, as a result of health systems with systemic health and social inequalities, people from racial and ethnic minority groups are at increased risk of getting sick and dying from COVID-19 in certain countries. These are crucial considerations that will be included in further studies and can point toward who, within a given age group, should get the vaccine first. We believe that these results can provide a quantification of the effectiveness of different allocation scenarios under four metrics of disease burden and can be used as an evidence-based guidance to vaccine prioritization.

SUPPLEMENTARY MATERIALS

Supplementary material for this article is available at http://advances.sciencemag.org/cgi/content/full/7/6/eabf1374/DC1

REFERENCES AND NOTES

1. Johns Hopkins University and Medicine, Coronavirus COVID-19 global cases by the Center for Systems Science and Engineering (CSSE) at Johns Hopkins University (JHU) (2020); https://coronavirus.jhu.edu/map.html.
2. A. Mullard, COVID-19 vaccine development pipeline gears up. *Lancet* **395**, 1751–1752 (2020).
3. C. Zimmer, J. Corum, S.-L. Wee, Coronavirus Vaccine Tracker (2020); https://www.nytimes.com/interactive/2020/science/coronavirus-vaccine-tracker.html.
4. R. Cohen, C. Jung, N. Ouldali, A. Sellam, C. Batard, F. Cahn-Sellem, A. Elbez, A. Wollner, O. Romain, F. Corrard, S. Aberrane, N. Soismier, R. Creidy, M. Smati-Lafarge, O. Launay, S. Bechet, E. Varon, C. Levy, Assessment of spread of SARS-CoV-2 by RT-PCR and concomitant serology in children in a region heavily affected by COVID-19 pandemic. *medRxiv* 2020.06.12.20129221 (2020).
5. A. D. Usher, COVID-19 vaccines for all? *Lancet* **395**, 1822–1823 (2020).
6. M. Twohey, Who Gets a Vaccine First? U.S. Considers Race in Coronavirus Plans (2020).
7. Centers for Disease Control and Prevention, 2009 H1N1 Flu (2009); www.cdc.gov/h1n1flu/vaccination/vaccinesupply.htm.
8. J. Zhang, M. Litvinova, Y. Liang, Y. Wang, W. Wang, S. Zhao, Q. Wu, S. Merler, C. Viboud, A. Vespignani, M. Ajelli, H. Yu, Changes in contact patterns shape the dynamics of the COVID-19 outbreak in China. *Science* **368**, 1481–1486 (2020).
9. Moderna, A phase 3, randomized, stratified, observer-blind, placebo-controlled study to evaluate the efficacy, safety, and immunogenicity mRNA-1273 SARS-CoV-2 vaccine in adults aged 18 years and older (2020).
10. Pfizer, A phase 1/2/3, placebo-controlled, randomized, observer-blind, dose-finding study to evaluate the safety, tolerability, immunogenicity, and efficacy of SARS-CoV-2 RNA vaccine candidates against COVID-19 in healthy individuals (2020), pp. 1–137.
11. CDC, COVID-19 Pandemic Planning Scenarios (2020); www.cdc.gov/coronavirus/2019-ncov/hcp/planning-scenarios.html.
12. N.M. Ferguson, D. Laydon, G. Nedjati-Gilani, N. Imai, K. Ainslie, M. Baguelin, S. Bhatia, A. Boonyasiri, Z. Cucunubá, G. Cuomo-Dannenburg, A. Dighe, I. Dorigatti, H. Fu, K. Gaythorpe, W. Green, A. Hamlet, W. Hinsley, L. C. Okell, S. van Elsland, H. Thompson, R. Verity, E. Volz, H. Wang, Y. Wang, Patrick GT Walker, C. Walters, P. Winskill, C. Whittaker, C. A. Donnelly, S. Riley, A. C. Ghani, Impact of non-pharmaceutical interventions (NPIs) to reduce COVID-19 mortality and healthcare demand (2020); https://doi.org/10.25561/77482.
13. Washington State Coronavirus Response, COVID-19 risk assessment dashboard (2020); https://coronavirus.wa.gov/what-you-need-know/covid-19-risk-assessment-dashboard.
14. State of California, COVID-19 data and tools (2020); https://covid19.ca.gov/data-and-tools/.
15. Centers for Disease Control and Prevention, Final estimates for 2009–10 seasonal influenza and influenza A (H1N1) 2009 monovalent vaccination coverage, August 2009 to May 2010 (2010); www.cdc.gov/flu/fluvaxview/coverage_0910estimates.htm.
16. Q.-L. Jing, M.-J. Liu, J. Yuan, Z.-B. Zhang, A.-R. Zhang, N. E. Dean, L. Luo, M. Ma, I. Longini, E. Kenah, Y. Lu, Y. Ma, N. Jalali, L.-Q. Fang, Z.-C. Yang, Y. Yang, Household secondary attack rate of COVID-19 and associated determinants. *medRxiv* 2020.04.11.20056010 (2020).
17. Q. Bi, Y. Wu, S. Mei, C. Ye, X. Zou, Z. Zhang, X. Liu, L. Wei, S. A. Truelove, T. Zhang, W. Gao, C. Cheng, X. Tang, X. Wu, Y. Wu, B. Sun, S. Huang, Y. Sun, J. Zhang, T. Ma, J. Lessler, T. Feng, Epidemiology and transmission of COVID-19 in 391 cases and 1286 of their close contacts in Shenzhen, China: A retrospective cohort study. *Lancet* **20**, 911–919 (2020).

18. F. P. Havers, C. Reed, T. Lim, J. M. Montgomery, J. D. Klena, A. J. Hall, A. M. Fry, D. L. Cannon, C.-F. Chiang, A. Gibbons, I. Krapiunaya, M. Morales-Betoulle, K. Roguski, M. A. U. Rasheed, B. Freeman, S. Lester, L. Mills, D. S. Carroll, S. M. Owen, J. A. Johnson, V. Semenova, C. Blackmore, D. Blog, S. J. Chai, A. Dunn, J. Hand, S. Jain, S. Lindquist, R. Lynfield, S. Pritchard, T. Sokol, L. Sosa, G. Turabelidze, S. M. Watkins, J. Wiesman, R. W. Williams, S. Yendell, J. Schiffer, N. J. Thornburg, Seroprevalence of antibodies to SARS-CoV-2 in 10 sites in the United States, March 23-May 12, 2020. *JAMA Intern. Med.* **180**, 1576–1586 (2020).
19. X. Lu, L. Zhang, H. Du, J. Zhang, Y. Y. Li, J. Qu, W. Zhang, Y. Wang, S. Bao, Y. Li, C. Wu, H. Liu, D. Liu, J. Shao, X. Peng, Y. Yang, Z. Liu, Y. Xiang, F. Zhang, R. M. Silva, K. E. Pinkerton, K. Shen, H. Xiao, S. Xu, G. W. K. Wong; Chinese Pediatric Novel Coronavirus Study Team, SARS-CoV-2 infection in children. *N. Engl. J. Med.* **382**, 1663–1665 (2020).
20. K.-Q. Kam, C. F. Yung, L. Cui, R. T. P. Lin, T. M. Mak, M. Maiwald, J. Li, C. Y. Chong, K. Nadua, N. W. H. Tan, K. C. Thoon, A well infant with coronavirus disease 2019 (COVID-19) with high viral load. *Clin. Infect. Dis.* **71**, 847–849 (2020).
21. N. G. Davies, A. J. Kucharski, R. M. Eggo, A. Gimma; CMMID COVID 19 working group, W. J. Edmunds, The effect of non-pharmaceutical interventions on COVID-19 cases, deaths and demand for hospital services in the UK: A modelling study. *Lancet* **5**, E375–E385 (2020).
22. S. A. Lauer, K. H. Grantz, Q. Bi, F. K. Jones, Q. Zheng, H. R. Meredith, A. S. Azman, N. G. Reich, J. Lessler, The incubation period of coronavirus disease 2019 (COVID-19) from publicly reported confirmed cases: Estimation and application. *Ann. Intern. Med.* **172**, 577–582 (2020).
23. Q. Li, X. Guan, P. Wu, X. Wang, L. Zhou, Y. Tong, R. Ren, K. S. M. Leung, E. H. Y. Lau, J. Y. Wong, X. Xing, N. Xiang, Y. Wu, C. Li, Q. Chen, D. Li, T. Liu, J. Zhao, M. Liu, W. Tu, C. Chen, L. Jin, R. Yang, Q. Wang, S. Zhou, R. Wang, H. Liu, Y. Luo, Y. Liu, G. Shao, H. Li, Z. Tao, Y. Yang, Z. Deng, B. Liu, Z. Ma, Y. Zhang, G. Shi, T. T. Y. Lam, J. T. Wu, G. F. Gao, B. J. Cowling, B. Yang, G. M. Leung, Z. Feng, Early transmission dynamics in Wuhan, China, of novel coronavirus-infected pneumonia. *N. Engl. J. Med.* **382**, 1199–1207 (2020).
24. N. M. Linton, T. Kobayashi, Y. Yang, K. Hayashi, A. R. Akhmetzhanov, S.-m. Jung, B. Yuan, R. Kinoshita, H. Nishiura, Incubation period and other epidemiological characteristics of 2019 novel coronavirus infections with right truncation: A statistical analysis of publicly available case data. *J. Clin. Med.* **9**, 538 (2020).
25. J. Qin, C. You, Q. Lin, T. Hu, S. Yu, X.-H. Zhou, Estimation of incubation period distribution of COVID-19 using disease onset forward time: A novel cross-sectional and forward follow-up study. *Sci. Adv.* **6**, eabc1202 (2020).
26. S. M. Bartsch, K. J. O'Shea, M. C. Ferguson, M. E. Bottazzi, S. N. Cox, U. Strych, J. A. McKinnell, P. T. Wedlock, S. S. Siegmund, P. J. Hotez, B. Y. Lee, How efficacious must a COVID-19 coronavirus vaccine be to prevent or stop an epidemic by itself. *medRxiv* 2020.05.29.20117184 (2020).
27. M. Makhoul, H. H. Ayoub, H. Chemaitelly, S. Seedat, G. R. Mumtaz, S. Al-Omari, L. J. Abu-Raddad, Epidemiological impact of SARS-CoV-2 vaccination: Mathematical modeling analyses. *medRxiv* 2020.04.19.20070805 (2020).
28. I. M. Longini, E. Ackerman, L. R. Elveback, An optimization model for influenza A epidemics. *Math. Biosci.* **38**, 141–157 (1978).
29. J. Medlock, A. P. Galvani, Optimizing influenza vaccine distribution. *Science* **325**, 1705–1708 (2009).
30. L. Matrajt, I. M. Longini Jr., Optimizing vaccine allocation at different points in time during an epidemic. *PLOS ONE* **5**, e13767 (2010).
31. F. J. Ibarrondo, J. A. Fulcher, D. Goodman-Meza, J. Elliott, C. Hofmann, M. A. Hausner, K. G. Ferbas, N. H. Tobin, G. M. Aldrovandi, O. O. Yang, Rapid decay of anti–SARS-CoV-2 antibodies in persons with mild covid-19. *N. Engl. J. Med.* **383**, 1085–1087 (2020).
32. Q.-X. Long, X.-J. Tang, Q.-L. Shi, Q. Li, H.-J. Deng, J. Yuan, J.-L. Hu, W. Xu, Y. Zhang, F.-J. Lv, K. Su, F. Zhang, J. Gong, B. Wu, X.-M. Liu, J.-J. Li, J.-F. Qiu, J. Chen, A.-L. Huang, Clinical and immunological assessment of asymptomatic SARS-CoV-2 infections. *Nat. Med.* **26**, 1200–1204 (2020).
33. Centers for Disease Control and Prevention, *Assessing Risk Factors for Severe COVID-19 Illness* (2020); https://www.cdc.gov/coronavirus/2019-ncov/covid-data/investigations-discovery/assessing-risk-factors.html.
34. European Centre for Disease and Prevention and Control, *COVID-19 Clusters and Outbreaks in Occupational Settings in the EU/EEA and the UK* (2020); www.ecdc.europa.eu/sites/default/files/documents/COVID-19-in-occupational-settings.pdf.
35. M. W. Hooper, A. M. Nápoles, E. J. Pérez-Stable, COVID-19 and racial/ethnic disparities. *JAMA* **323**, 2466–2467 (2020).
36. L. S. Muñoz-Price, A. B. Nattinger, F. Rivera, R. Hanson, C. G. Gmehlin, A. Perez, S. Singh, B. W. Buchan, N. A. Ledeboer, L. E. Pezzin, Racial disparities in incidence and outcomes among patients with COVID-19. *JAMA Netw. Open* **3**, e2021892 (2020).
37. United States Census Bureau, *Washington* (2020); https://data.census.gov/cedsci/profile?q=Washington&g=0400000US53.
38. Population Pyramid, *Population of United States of America 2020* (2020); www.populationpyramid.net/united-states-of-america/2020/.
39. K. Prem, A. R. Cook, M. Jit, Projecting social contact matrices in 152 countries using contact surveys and demographic data. *PLOS Comput. Biol.* **13**, e1005697 (2017).
40. Z. Du, X. Xu, Y. Wu, L. Wang, B. J. Cowling, L. A. Meyers, The serial interval of COVID-19 from publicly reported confirmed cases. *Emerg. Infect. Dis.* **26**, 1341–1343 (2020).
41. H. Nishiura, N. M. Linton, A. R. Akhmetzhanov, Serial interval of novel coronavirus (COVID-19) infections. *Int. J. Infect. Dis.* **93**, 284–286 (2020).
42. M. E. Halloran, M. Haber, I. M. Longini, Interpretation and estimation of vaccine efficacy under heterogeneity. *Am. J. Epidemiol.* **136**, 328–343 (1992).
43. M. E. Halloran, I. M. Longini, C. J. Struchiner, *Design and Analysis of Vaccine Studies* (Springer, 2010).
44. C. Audet, W. Hare, *Derivative-Free and Blackbox Optimization* (Cham, Switzerland, Springer, 2017).
45. The Sage Developers, *SageMath, the Sage Mathematics Software System (Version 9.1)* (2020); www.sagemath.org.
46. S. Kotz, N. Balakrishnan, N.L. Johnson, *Continuous Multivariate Distributions* (Models and Applications, Wiley, 2000), vol. 1.
47. F. Gao, L. Han, Implementing the Nelder-Mead simplex algorithm with adaptive parameters. *Comput. Optimiz. Appl.* **51**, 259–277 (2012).
48. P. Virtanen, T. E. Oliphant, M. Haberland, T. Reddy, D. Cournapeau, E. Burovski, P. Peterson, W. Weckesser, J. Bright, S. J. van der Walt, M. Brett, J. Wilson, K. J. Millman, N. Mayorov, A. R. J. Nelson, E. Jones, R. Kern, E. Larson, C. J. Carey, İ. Polat, Y. Feng, E. W. Moore, J. V. Plas, D. Laxalde, J. Perktold, R. Cimrman, I. Henriksen, E. A. Quintero, C. R. Harris, A. M. Archibald, A. H. Ribeiro, F. Pedregosa, P. van Mulbregt; SciPy 1.0 Contributors, SciPy 1.0: Fundamental algorithms for scientific computing in python. *Nat. Methods* **17**, 261–272 (2020).
49. J. Kennedy, R. Eberhart, Particle swarm optimization. *Proc. IEEE Int. Conf. Neural Net.* **4**, 1942–1948 (1995).
50. L. J. V. Miranda, PySwarms: A research toolkit for Particle Swarm Optimization in Python. *J. Open Source Soft.* **3**, 433 (2018).
51. W. E. Wei, Z. Li, C. J. Chiew, S. E. Yong, M. P. Toh, V. J. Lee, Presymptomatic transmission of SARS-CoV-2—Singapore. *Morb. Mortal. Wkly. Rep.* **69**, 411–415 (2020).
52. Y.-H. Lee, C. M. Hong, D. H. Kim, T. H. Lee, J. Lee, Clinical course of asymptomatic and mildly symptomatic patients with coronavirus disease admitted to community treatment centers, South Korea. *Emerg. Infect. Dis.* **26**, 2346–2352 (2020).
53. K. Mizumoto, K. Kagaya, A. Zarebski, G. Chowell, Estimating the asymptomatic proportion of coronavirus disease 2019 (COVID-19) cases on board the Diamond Princess cruise ship, Yokohama, Japan, 2020. *Euro Surveillance* **25**, 2000180 (2020).
54. X. He, E. H. Y. Lau, P. Wu, X. Deng, J. Wang, X. Hao, Y. C. Lau, J. Y. Wong, Y. Guan, X. Tan, X. Mo, Y. Chen, B. Liao, W. Chen, F. Hu, Q. Zhang, M. Zhong, Y. Wu, L. Zhao, F. Zhang, B. J. Cowling, F. Li, G. M. Leung, Temporal dynamics in viral shedding and transmissibility of COVID-19. *Nat. Med.* **26**, 672–675 (2020).
55. J. T. Wu, K. Leung, G. M. Leung, Nowcasting and forecasting the potential domestic and international spread of the 2019-nCoV outbreak originating in Wuhan, China: A modelling study. *Lancet* **395**, 689–697 (2020).
56. S. Zhao, Q. Lin, J. Ran, S. S. Musa, G. Yang, W. Wang, Y. Lou, D. Gao, L. Yang, D. He, M. H. Wang, Preliminary estimation of the basic reproduction number of novel coronavirus (2019-nCoV) in China, from 2019 to 2020: A data-driven analysis in the early phase of the outbreak. *Int. J. Infect. Dis.* **92**, 214–217 (2020).

Acknowledgments: L.M. acknowledges M. Moore for helpful discussions regarding the model structure and B. E. McGough for help with cluster computing. **Funding:** This work was supported by the National Institute of Allergy and Infectious Diseases, 1 UM1 AI148684-01 (L.M., T.L., and E.R.B.). Scientific Computing Infrastructure at Fred Hutchinson Cancer Research Center was funded by NIH ORIP grant S10OD028685. **Author contributions:** L.M. and E.R.B. conceived the study. L.M. developed the model. L.M. and J.E. wrote the optimization algorithms. L.M. and T.L. analyzed the data. L.M. produced the first draft of the manuscript. All authors contributed to the final draft. **Competing interests:** The authors declare that they have no competing interests. **Data and materials availability:** All data needed to evaluate the conclusions in the paper are present in the paper and/or the Supplementary Materials. Code is available at https://github.com/lulelita/vaccine_optimization. Additional data related to this paper may be requested from the authors.

Submitted 6 October 2020
Accepted 17 December 2020
Published 3 February 2021
10.1126/sciadv.abf1374

Citation: L. Matrajt, J. Eaton, T. Leung, E. R. Brown, Vaccine optimization for COVID-19: Who to vaccinate first?. *Sci. Adv.* **7**, eabf1374 (2021).

Vaccine optimization for COVID-19: Who to vaccinate first?

Laura MatrajtJulia EatonTiffany LeungElizabeth R. Brown

Sci. Adv., 7 (6), eabf1374. • DOI: 10.1126/sciadv.abf1374